Effects of Corrosion on Degradation of Tensile Strength of Steel Bridge Members

J.M. Ruwan S. Appuhamy[1],
[1]Department of Civil & Environmental Engineering, Ehime University, Japan
(ruwan@cee.ehime-u.ac.jp)
Mitao Ohga[2],
[2]Department of Civil & Environmental Engineering, Ehime University, Japan
(ohga@cee.ehime-u.ac.jp)
Pang-jo Chun[3],
[3]Department of Civil & Environmental Engineering, Ehime University, Japan
(chun.pang-jo.mj@ehime-u.ac.jp)
Seiji Furukawa[4],
[4]West Nippon Expressway Engineering Shikoku, Japan
(seiji.furukawa@w-e-shikoku.co.jp)
P.B. Ranjith Dissanayake[5],
[5]Department of Civil Engineering, University of Peradeniya, Sri Lanka
(ranjith@civil.pdn.ac.lk)

Abstract

Evaluation of existing steel bridges becomes vital due to natural aging, increasing load spectra, deterioration caused by corrosion, increasing seismic demand, and other problems. In the result, bridge structures exposed to aggressive environmental conditions are subjected to time-variant changes of resistance. Corrosion becomes one of the major causes of deterioration of steel bridges and there have been many damage examples of older steel bridge structures due to corrosion around the world during past few decades. Controlling corrosion on bridge structures can prevent premature failure and lengthen their useful service life, both of which save money and natural resources, and promote public safety. Therefore, understanding of the influence of damage due to corrosion on the remaining load-carrying capacities is a vital task for the maintenance management of steel highway infrastructures.

But at the moment, number of steel railway and highway bridge infrastructures in the world is steadily increasing as a result of building new steel structures and extending the life of older structures. Therefore, it would be an exigent task to measure several thousands of points, to accurately reproduce the corroded surface by numerical methods and to predict the behaviour of that corroded member more precisely. So, there is a need of more brisk and accurate assessment method which can be used to make reliable decisions affecting the cost and safety. Therefore, this paper presents the analytical results of many actual corroded steel members and comparison of them with their respective experimental results. Further, a simple and reliable analytical method by measuring only the maximum corroded depth ($t_{c,max}$) is proposed, in order to predict the residual strength capacities of corroded steel plates more accurately.

Keywords: Bridge maintenance, Corrosion, Remaining strength, FEM analysis

1.0 Introduction

Since the initiation of construction of first steel bridges around 200 years ago, steel has instituted itself worldwide in the 19th and 20th centuries and in a multiplicity of bridge constructions as best building material. This is due to the fact that opposing to concrete it has a better strength to weight relationship. With steel, the construction of bridges becomes easier with shorter construction time and reduced construction costs. However, the disadvantage is the unprotected structural steel in the atmosphere subjects to corrosion which leads to the reduction of their carrying capacities. Therefore, a reliable maintenance of steel bridges is crucial as these bridges have to ensure smooth traffic for cars, trucks as well as rails which represent the most important mediums for the transportation of goods and services in our modern society. Therefore, it is very important to understand the behaviour of existing bridges which are corroding for decades and establish an accurate methodology to estimate the remaining load carrying capacities for proper maintenance of steel highway and railway infrastructures, ensuring their safety.

Corrosion is a time-based process of deterioration of a material as a result of a reaction with its environment. In this electrochemical process, initial attack occurs at anodic areas on the surface, where ferrous ions go into solution. Electrons are released from the anode and move through the metallic structure to the adjacent cathodic sites on the surface, where they combine with oxygen and water to form hydroxyl ions. These react with the ferrous ions from the anode to produce ferrous hydroxide, which itself is further oxidized in air to produce hydrated ferric oxide (i.e. red rust). The sum of these reactions can be represented by the following equation:

$$4Fe + 3O_2 + 2H_2O = 2Fe_2O_3.H_2O \tag{1}$$
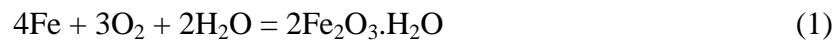
(Steel) + (Oxygen) + (Water) = Hydrated ferric oxide (Rust)

This process requires the simultaneous presence of water and oxygen. In the absence of either, corrosion does not occur. The consequences of corrosion are many and varied and the effects of these on the safe, reliable and efficient operation of structures are often considered than simply losing a volume of metal. One of the major harmful effects of corrosion is the reduction of metal thickness leading to loss of mechanical strength and structural failure, causing severe disastrous and hazardous injuries to people. There are more than 50,000 steel railway bridges in Japan, where more than half of them have been used over 60 years and some bridges are aged over 100 years. With aging, Corrosion becomes one of the major causes of deterioration of steel bridges, and its' damages seriously affect on the durability of steel bridges (Fujii, 2003 and Rahgozar, 2009).

Benefits of regular and proper inspections of older bridges cannot be overlooked. They not only help in planning the necessary work but also help in discovering and monitoring any problems, thereby reducing expensive maintenance, reducing operating hazards, preventing structural failures and averting emergencies. Therefore, no laxness in inspections should be permitted as they form the essential source of information to carry out a comprehensive evaluation of its current capacity. Several experimental studies and detailed investigations of corroded surfaces were done by some researchers during the past few decades, in order to introduce methods of

estimating the remaining strength capacities of corroded steel plates (Matsumoto, 1989; Muranaka, 1998; Kariya, 2003; Kaita, 2011). But, to develop a more reliable strength estimation technique, only experimental approach is not enough as actual corroded surfaces are different from each other. Further, due to economic constraints, it is not possible to conduct tests for each and every aged bridge structure within their bridge budgets. Therefore, nowadays, use of numerical analysis method could be considered to have a reliable estimation in bridge infrastructure maintenance industry (Kaita, 2008).

Further, Ahmmad *et al.* (2010) investigated the deformability of corroded steel plates under quasi-static uniaxial tension through both experimental and numerical analyses. They proposed empirical formulae to estimate the reduction in deformability and energy absorption capacity due to pitting corrosion and general corrosion under uniaxial tension. Ok *et al.* (2007) carried out the nonlinear finite element analyses of panels with various locations and sizes of pitting corrosion and multi-variable regression method is applied to derive new formulae to predict ultimate strength of unstiffened plates with localized corrosion. Therefore it can be seen that the finite element analysis method has now become the most common, powerful and flexible tool in rational structural analysis and makes it possible to predict the strength of complex structures more accurately than existing classical theoretical methods.

But, a simple and efficient methodology to estimate the residual strength of aged steel bridge infrastructures is deemed necessary, as it is not easy to measure several thousands of points in order to accurately reproduce the corroded surface by numerical methods and to predict the behaviour of that corroded member more precisely. Therefore, the analytical results of many actual corroded steel members and comparison of them with their respective experimental results are presented in this paper, in order to investigate the applicability of numerical modelling approach for residual strength estimations of corroded steel members. Further, the feasibility of establishing of a simple, accurate and reliable analytical method to predict the residual strength capacities of a corroded steel member by measuring only the maximum corroded depth ($t_{c,max}$) is also discussed.

2.0 Tensile Test of Corroded Specimens

2.1 Test Specimen Configuration

The tensile test specimens used for this study were cut out from a steel girder of Ananai River Bridge in Kochi Prefecture on the shoreline of the Pacific Ocean, which had been used for about hundred years. This bridge had simply supported steel plate girders with six spans, with each of 13.5m and it was constructed as a railway bridge in 1900, and in 1975 changed to a pedestrian bridge, when the reinforced concrete slab was cast on main girders. The bridge was dismantled due to serious corrosion damage in year 2001. Many severe corrosion damages distributed all over the girder, especially, large corrosion pits or locally-corroded portions were observed on upper flanges and its cover plates. Then, 21 (F1-F21) and 5 (W1-W5) test specimens were cut out from the cover plate on upper flange and web plate respectively.

Before conducting the thickness measurements, all rusts over both surfaces were removed carefully by using the electric wire brushes and punches. Then, two new SM490A plates (t=16mm) were jointed to both sides of specimen by the butt full penetration welding for grip parts to loading machine, as shown in Figure 1. Here, the flange and web specimens have the widths ranged from 70-80mm and 170-180mm respectively. The test specimen configuration is shown in Figure 1. In addition, 4 corrosion-free specimens (JIS5 type) were made of each two from flange and web, and the tensile tests were carried out in order to clarify the material properties of test specimens. The material properties obtained from these tests are shown in Table 1.
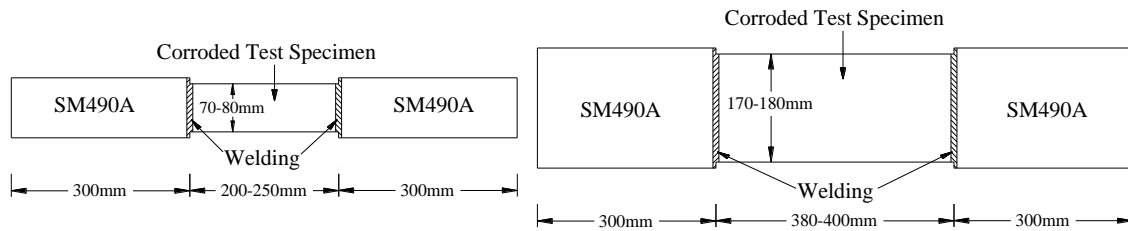
Figure 1: Dimensions of test specimens

Table 1: Material properties

Specimen	Elastic modulus /(GPa)	Poisson's ratio	Yield stress /(MPa)	Tensile strength /(MPa)	Elongation at breaking /(%)
Corrosion-free plate (flange)	187.8	0.271	281.6	431.3	40.19
Corrosion-free plate (web)	195.4	0.281	307.8	463.5	32.87
SS400 JIS	200.0	0.300	245~	400~510	–

2.2 Corrosion Surface Measurement

Accuracy and convenience are highly demanded in the measurement of corrosion surface irregularities. Furthermore, portability, good operability and lightness would be also imperative for choosing of a measurement device for on-site measurements. Therefore, the portable 3-dimentional scanning system, which can measure the 3-dimentional coordinate values at any arbitrary point on the corrosion surface directly and continuously, was used for the measurement of surface irregularities of the test specimens. Here, the thickness of the corroded surface can be calculated easily from those measured coordinates. The measuring device has three arms and six rotational joints, and can measure the coordinates of a point on steel surface by using the non-contact scanning probe (laser line probe). The condition of thickness measurement is shown in Figure 2. Since this probe irradiates the steel surface with a laser beam, which has about 100mm width, the large number of 3-dimensional coordinate data can be obtained easily at a time. So, the thicknesses of all scratched specimens were measured by

using this 3D laser scanning device and the coordinate data was obtained in a grid of 0.5mm intervals in both X and Y directions. Then, the remaining thicknesses of all grid points were calculated by using the difference of the coordinate values of both sides of those corroded specimens. Then, the statistical thickness parameters such as average thickness (t_{avg}), minimum thickness (t_{min}), standard deviation of thickness (σ_{st}) and coefficient of variability (CV) were calculated from the measurement results.

Figure 2: Condition of thickness measurement

2.3 Corrosion Level Classification

It is necessary to categorize the different corrosion conditions which can be seen in actual steel structures, into few general types for better understanding of their remaining strength capacities considering their visual distinctiveness, amount of corrosion and their expected mechanical and ultimate behaviours. The Figure 3 shows the relationship between the nominal ultimate stress ratio (σ_{bn}/σ_b) and the minimum thickness ratio (μ), where σ_{bn} is the nominal ultimate stress and σ_b is the ultimate stress of corrosion-free plate. Here, the minimum thickness ratio (μ) is defined as:

$$\mu = \frac{t_{min}}{t_0} \tag{2}$$

There, the initial thickness (t_0) of the flange specimens and web specimens are 10.5mm and 10.0mm respectively. Therefore, three different types of corrosion levels were identified according to their severity of corrosion and they are classified accordingly as follows:

$\mu > 0.75$; Minor Corrosion
$0.75 \geq \mu \geq 0.5$; Moderate Corrosion
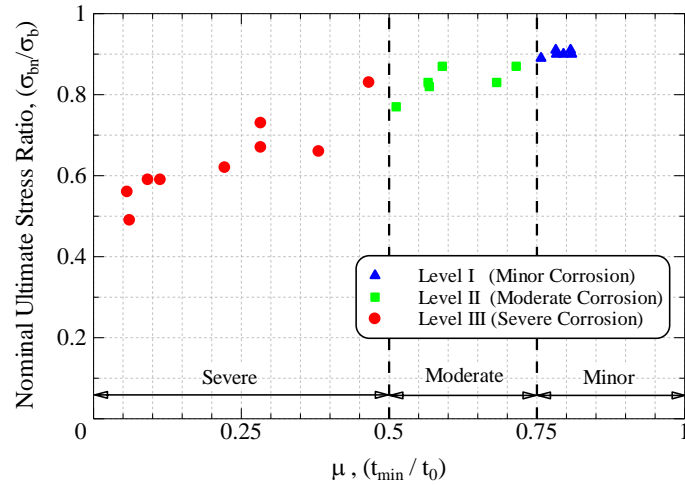$\mu < 0.5$; Severe Corrosion

Figure 3: Relationship of ultimate stress ratio & minimum thickness ratio (μ)

2.4 Experimental Results

Tensile loading tests were carried out at constant velocity under loading control by using a hydraulic loading test machine (maximum load: 2940KN) for all 26 specimens with different corrosion conditions. The loading velocity was set to 200N/sec for minor corroded specimens and 150N/sec for moderate and severe corroded specimens. Figure 4 shows the load-displacement curves of specimens F-14, F-13 and F-19 with 3 corrosion types. Herein, the specimen (F-14) with minor corrosion has almost same mechanical properties (such as apparent yield strength and load-displacement behavior etc.) as the corrosion-free specimen. On the other hand, the moderate corroded specimen (F-13) and the severe corroded specimen (F-19) show obscure yield strength and the elongation of the specimen F-19 decreases notably. The reason for this is believed to be that the local section with a small cross-sectional area yields at an early load stage because of the stress concentration due to irregularity of corroded steel plate which elongates locally and reach to the breaking point.
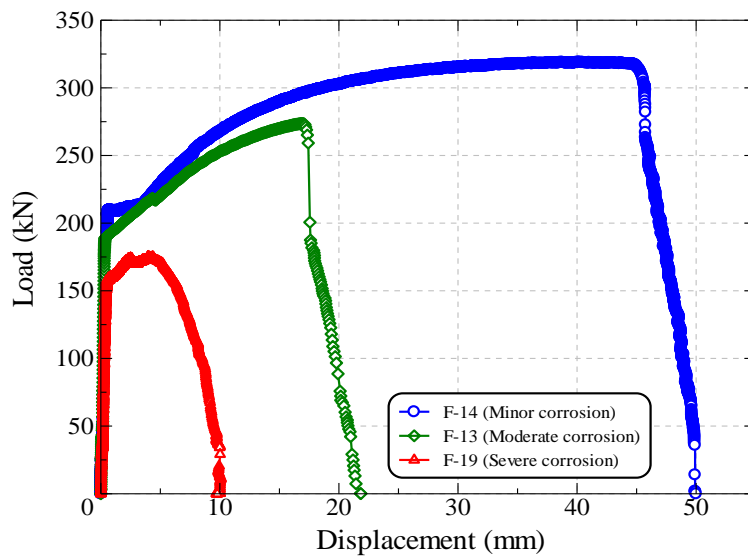

Figure 4: Load-displacement curves

3.0 Numerical Analysis

3.1 Analytical Model

The 3D isoparametric hexahedral solid element with eight nodal points (HX8M) and updated Lagrangian method based on incremental theory were adopted in these analyses. Non linear elastic-plastic material, Newton-Raphson flow rule and Von Mises yield criterion were assumed for material properties. Further, an automatic incremental-iterative solution procedure was performed until they reached to the pre-defined termination limit.

The analytical models with different length (L) and width (W) dimensions were modeled with their respective corrosion conditions as shown in Figure 5. 2mm regular mesh pattern was adopted for all analytical models. One edge of the member's translation in X, Y and Z directions were fixed and only the Y and Z direction translations of the other edge (loading edge) were fixed to simulate with the actual experimental condition. Then the uniform incremental displacements were applied to the loading edge. Yield stress σy = 294.7 [MPa], Elastic modulus E = 191.6 [GPa], Poisson's ratio ν = 0.276 were applied to all analytical models, respectively.
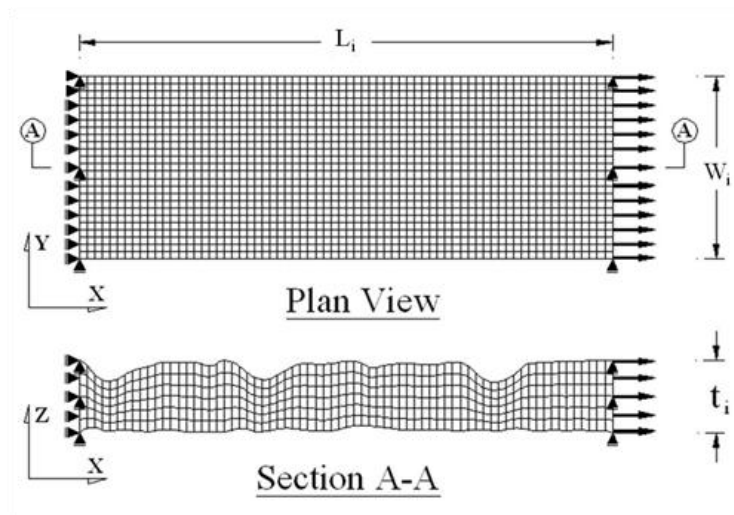

Figure 5: Analytical model of corroded member

3.2 Ductile Fracture Criterion

The Stress Modified Critical Strain Model (SMCS)' was proposed by Kavinde et al. (2006), to evaluate the initiation of ductile fracture as a function of multiaxial plastic strains and stresses. This method was adopted in this analytical study. In SMCS criterion, the critical plastic strain ($\varepsilon_P^{Critical}$) is determined by the following expression:

$$\varepsilon_P^{Critical} = \alpha \cdot Exp\left(-1.5\frac{\sigma_m}{\sigma_e}\right) \qquad (3)$$

Where, α is toughness index and the stress triaxiality T = (σ_m / σ_e), a ratio of the mean or hydrostatic stress (σ_m) and the effective or Von Mises stress (σ_e). The toughness index α is a fundamental material property and hence obtained from the tensile test conducted for the non corroded specimen. The ultimate strength of each corroded specimen was calculated accordingly by using the SMCS criterion and compared with their experimental ultimate capacities to understand the feasibility of the numerical modeling approach for remaining strength estimation of corroded steel plates.

3.3 Analytical Results

First, analytical modeling of the non-corroded specimen was done with above described modeling and analytical features to understand the accuracy of the adopted procedure. It was found that the analytical model results were almost same as the experimental results with having a negligible percentage error of 0.03% and 0.02% in yield and tensile strengths respectively. Then, all other experimentally successful specimens were modeled accordingly and their yield and ultimate strengths were compared with the experimentally obtained values.

Figure 6 shows comparison of experimental and analytical the load-displacement curves of three specimens F-14, F-13 and F-19 with minor, moderate and severe corrosion conditions respectively. There, it can be seen that a very good agreement of experimental and analytical load-displacement behaviors for all 3 classified corrosion types can be obtained. Here, the percentage errors in yield and tensile strength predictions of the analytical models of three corrosion types are 0.53% and 0.03% in F-14, 2.96% and 0.70% in F-13 and 3.20% and 5.53% in F-19 respectively. Therefore, it is revealed that this analytical method can be used to predict the yield and tensile strength of actual corroded specimens more precisely.

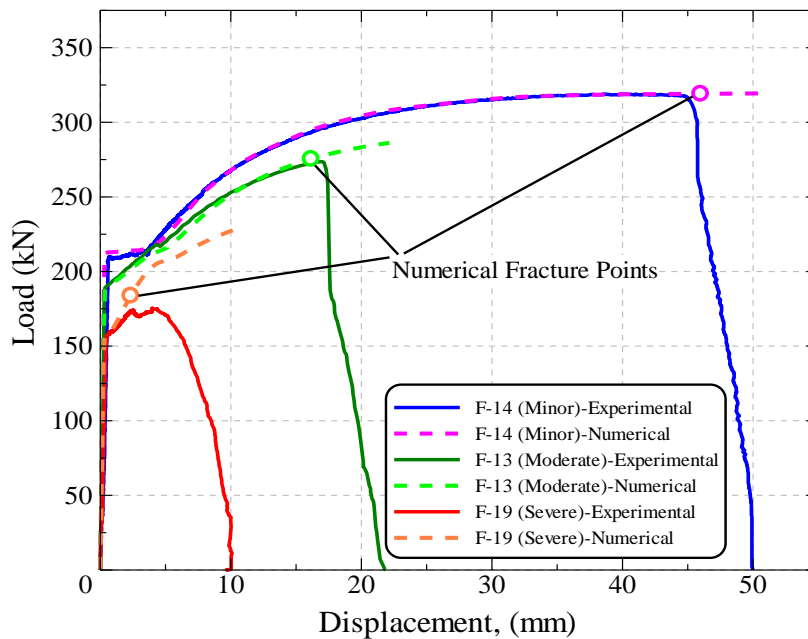
Figure 6:   Comparison

of experimental and analytical load-displacement curves

Further, Figure 7 shows the stress distribution at ultimate load and the failure surfaces of three different specimens F-14, F-13 and F-19. Here the failure surface was obtained from the most narrowed location of the deformed shape of the analytical model. It can be seen that the failure surfaces obtained from the analytical method and the experimental analysis indicated a very good comparison for all three corrosion categories and hence this fact too signifies the accuracy of the adopted numerical modelling method and SMCS fracture criterion.
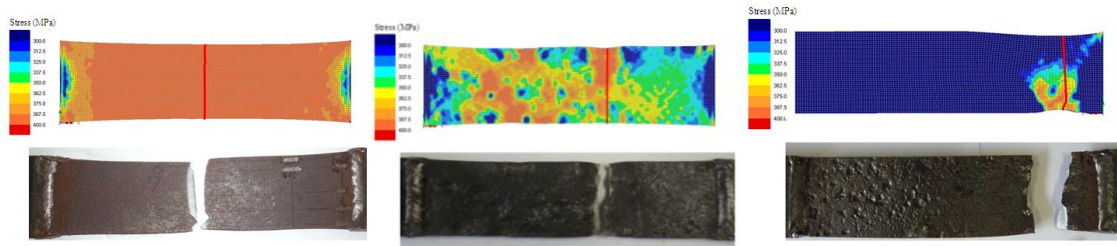
(a) F-14 [Minor corrosion]   (b) F-13[Moderate corrosion]   (c) F-19 [Severe corrosion]

Figure 7: Stress distribution of the corroded specimens at ultimate load

4.0 Development of Brisk Analytical Method

4.1 Corrosion Condition Modelling (CCM) Parameters

It will be an exigent task to conduct detail corroded surface measurements for all aged steel infrastructures as the number of steel structures are steadily increasing in the world. Therefore, a simple, accurate and brisk method is deemed necessary to model different corroded surfaces numerically and predict their yield and ultimate behaviors. So, in this study, two parameters were defined to model the corroded surface considering the stress concentration effect and to obtain the yield and ultimate behaviors more accurately. The following Figure 8(a) shows the variation of diameter of the maximum corroded pit vs. maximum corroded depth ($t_{c,max}$) and Figure 8(b) shows the normalized average thickness (t_{avg}/t_0) vs. normalized maximum corroded depth ($t_{c,max}/t_0$). Both Figures show a very good linear relationship and hence these parameters were used to develop an analytical model which can be used to predict the yield and ultimate behaviors of corroded steel plates with different corrosion conditions.

Therefore, by considering the Figure 8(a) and (b), the two equations for the corrosion condition modeling (CCM) parameters can be defined as:

$$D^* = 5.2 \, t_{c,max} \tag{4}$$

$$t^*_{avg} = t_0 - 0.2 \, t_{c,max} \tag{5}$$

where D^* and t^*_{avg} are the representative diameter of maximum corroded pit and representative average thickness respectively.
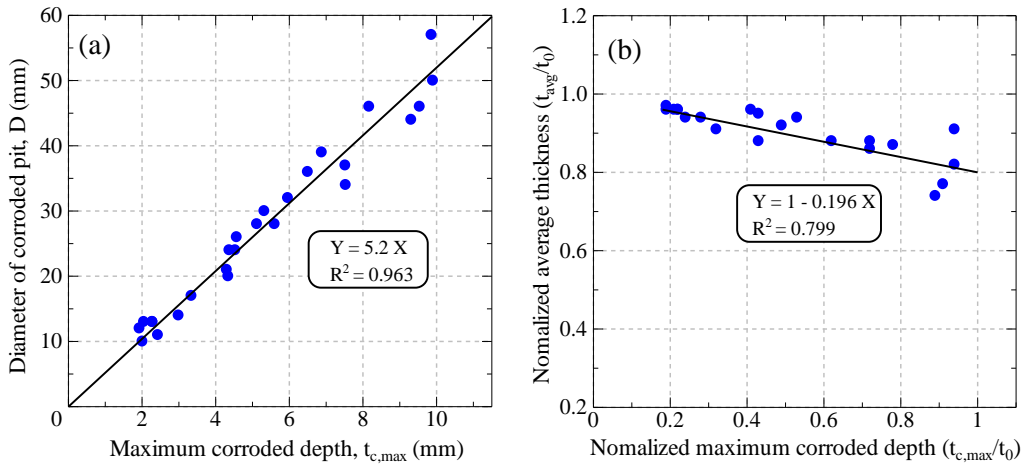
Figure 8: Relationship of (a) D vs. $t_{c,max}$ and (b) normalized t_{avg} vs. $t_{c,max}$

4.2 Brisk Analytical Model

The Figure 9 shows the analytical model, which is developed with the above CCM parameters for each corroded specimen with different corrosion conditions. Here, the maximum corroded pit was modelled by using the representative diameter (D^*) which could account the stress concentration effect and the material loss due to corrosion was considered by using the representative average thickness parameter (t_{avg}^*). The same modelling features and analytical procedure as described in section 3 were adopted for the analyses. Then the results of this model were compared with the experimental results to understand the effectiveness of the proposed model.
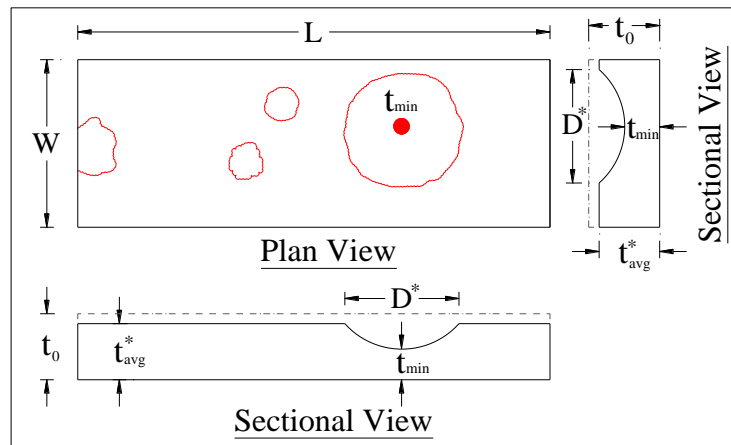

Figure 9: Analytical model with CCM parameters

4.3 Analytical Results

The Figure 10 shows the load-displacement behavior of 3 members F-14, F-13 and F-19 with minor, moderate and severe corrosion conditions respectively. It was revealed that a very good comparison of the load-displacement behavior can be seen for the all three classified corrosion types for the proposed analytical model too. Here, the percentage errors in yield and tensile strength predictions of the proposed analytical model for the three corrosion types are 0.13% and 0.83% in F-14, 0.38% and 1.01% in F-13 and 3.51% and 2.69% in F-19 respectively. Therefore it can be comprehended that the adopted method and the proposed analytical model can be used to predict the yield and ultimate behaviors precisely. Further, the failure surfaces and the stress distribution of different specimens with proposed analytical model at ultimate load are shown in Figure 11. There, it was noticed that a very good agreement of the failure surfaces of experimental and proposed model can be obtained too.
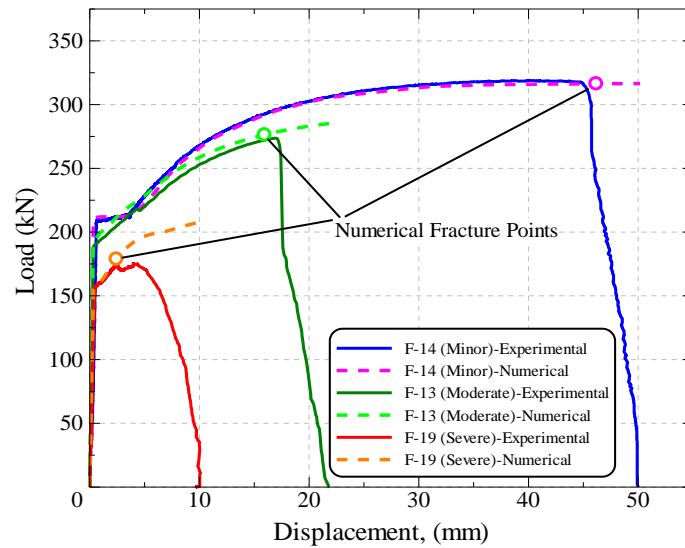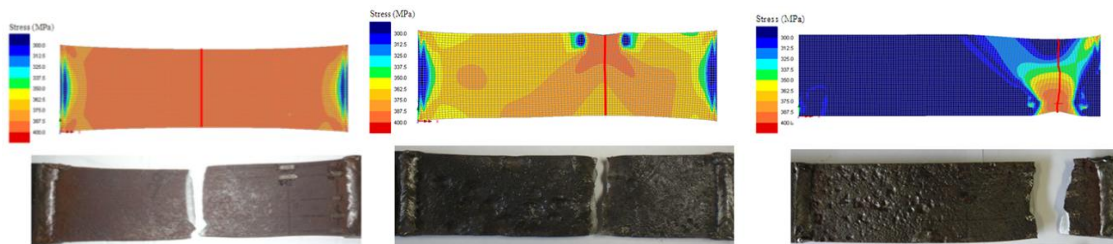

Figure 10: Comparison of load-displacement curves of experimental & proposed analytical model

(a) F-14 [Minor corrosion]   (b) F-13[Moderate corrosion]   (c) F-19 [Severe corrosion]

Figure 11: Stress distribution of the proposed analytical models of different specimens at ultimate load

Further, the comparison of 2mm model and the proposed model revealed that the stress distribution at ultimate load is almost same for minor corrosion members and small differences exist can be seen for moderate and severe corrosion members. The reason for this could be due to the differences of corroded surface irregularities in both models. Therefore it is evident that the use of the proposed analytical model with CCM parameters can estimate the remaining strength capacities of corroded steel members more easily and accurately.

5.0 Conclusions

1. A very good agreement between experimental and non linear FEM results can be seen for all three classified corrosion types. Further, their failure surfaces showed a good comparison with the experimental results too. So, the adopted numerical modeling technique can be used to predict the remaining strength capacities of actual corroded members accurately.

2. Two good relationships for the corrosion condition modeling (CCM) parameters can be defined as:

$$D^* = 5.2\ t_{c,max}$$
$$t^*_{avg} = t_0 - 0.2\ t_{c,max}$$

And the proposed analytical model with CCM parameters showed a very good agreement with the experimental results for all three classified corrosion types.

3. Further, the proposed analytical method is simple and gives more accurate remaining strength estimation of corroded steel plates and hence this analytical model can be used as a reliable and brisk method for the maintenance management of corroded steel infrastructures.

References

Ahmmad M.M. and Sumi Y. (2010), "Strength and Deformability of Corroded Steel Plates under Quasi-static Tensile Load", *Journal of Marine Science and Technology*, **15**, pp. 1-15

Fujii K., Kaita, T., Nakamura H. and Okumura M. (2003), "A Model Generating Surface Irregularities of Corroded Steel Plate for Analysis of Remaining Strength in Bridge Maintenance", *EASEC-9*, **9**, pp. 32-38

Kaita T., Appuhamy J.M.R.S., Ohga M. and Fujii K. (2011), "Estimation of Effective Thickness of Corroded Steel Plates for Remaining Strength Prediction", *Asset Management and Maintenance Journal (AMMJ)*, **24(3)**, pp. 38-45

Kaita T., Kawasaki Y., Isami H., Ohga M. and Fujii K. (2008), "Analytical Study on Remaining Compressive Strength and Ultimate Behaviours for Locally-corroded Flanges", *Proc. of EASEC-11*, Taiwan

Kariya A., Tagaya K., Kaita T. and Fujii K. (2003), "Basic Study on Effective Thickness of Corroded Steel Plate and Material Property", *Annual Conference of JSCE*, pp. 967-968

Kavinde A.M. and Deierlein G.G. (2006), "Void Growth Model and Stress Modified Critical Strain Model to Predict Ductile Fracture in Structural Steels", *Journal of Structural Engineering*, **132(12)**, pp. 1907-1918

Matsumoto M., Shirai Y., Nakamura I. and Shiraishi N. (1989), "A Proposal of Effective Thickness Estimation Method of Corroded Steel Member", *Bridge Foundation Engineering*, **23(12)**, pp. 19-25

Muranaka A., Minata O. and Fujii K. (1998), "Estimation of Residual Strength and Surface Irregularity of the Corroded Steel Plates", *Journal of Structural Engineering*, **44A**, pp. 1063-1071

Ok D., Pu Y. and Incecik A. (2007), "Computation of Ultimate Strength of Locally Corroded Unstiffened Plates under Uniaxial Compression", *Marine Structures*, **20**, pp. 100-114

Rahgozar R. (2009), "Remaining Capacity Assessment of Corrosion Damaged Beams using Minimum Curves", *Journal of Constructional Steel Research*, **65**, pp. 299-307